International Journal for Housing Science and Its Applications
Publish August 6, 2025. Volume 46, Issue 3 Pages 4850-4863

https://doi.org/10.70517/ijhsa463415

Research on permanent magnet switch design based on simulated annealing and structure optimization algorithm

Chunxiao Li[1,*], Wenxuan Wang[1] and Xin Li[1]
[1] State Grid Cangzhou Electric Supply Company, Cangzhou, Hebei, 061000, China
Corresponding authors: (e-mail: 18031991855@163.com).

Abstract The permanent magnet switch structure plays a crucial role in enhancing the efficient operation of permanent magnet linear motors. Based on this, this paper constructs a finite element simulation model of the permanent magnet switch structure based on the working principle of the permanent magnet switch, on the basis of analyzing the stray parameter and magnetic circuit model of the permanent magnet switch, and combining with Infolytica MagNet simulation software. Then from the multi-objective optimization problem of the permanent magnet switch structure, the multi-objective optimization model of the permanent magnet switch is established based on the optimization objectives and constraints. The genetic algorithm is introduced to optimize the parameters of the simulated annealing algorithm, and the multi-objective optimization model of permanent magnet switch is solved by GA-SA algorithm. Simulation shows that the GA-SA algorithm is relatively efficient, and the sinusoidal distortion rates of the cogging torque and the no-load air-gap magnetic density waveform are 0.32N-m and 21.75%, respectively, after solving the multi-objective optimization model. The optimized permanent magnet switch opening speed and opening coil energy conversion rate are increased by 21.92% and 20.80%, respectively. In conclusion, the permanent magnet switch design obtained by the multi-objective optimization algorithm meets the requirements of the permanent magnet linear motor and can significantly enhance the operating efficiency of the permanent magnet linear motor.

Index Terms permanent magnet switch design, magnetic circuit model, simulated annealing algorithm, multi-objective optimization model

I. Introduction

With the rapid development of the power system, the intelligence of the power grid has become an inevitable trend in the development of the power grid. Circuit breaker is an indispensable part of the power system, the intelligence of the switch and to a certain extent determines the degree of intelligence of the power grid [1]. So the intelligence of the power grid on the switch action reliability requirements continue to improve, so that the smart grid optimization operation and self-healing control, it requires that the switch can be in the power system failure, under the cooperation of the protection device can quickly and reliably cut off the fault current, to prevent the further deterioration of the accident, so as to ensure the stable operation of the power system [2]-[4]. When the switch in the capacitor bank, no-load transformer, no-load line, etc. casting and cutting operation, may produce a huge over-voltage and over-current, which will have a serious impact on the life and insulation of the equipment itself, the secondary protection equipment, so the intelligent switch in the realization of the synchronous phase-selective splitting and closing at the same time, but also must be a real-time monitoring of the system's various operating quantities, so as to reduce or eliminate the above impact [5]-[7].

The operating performance of the synchronous switch is affected by the closing and splitting time of the permanent magnet vacuum circuit breaker, while factors such as the switch control voltage, ambient temperature, and the degree of mechanical aging simultaneously affect the closing and splitting time of the switch [8]. Therefore, the traditional synchronous switch control technology usually uses voltage compensation, temperature compensation, mechanical compensation and other methods to reduce the influence of external environmental factors on the synchronous switch operating time [9]-[11]. However, the traditional open-loop compensation control methods generally need to carry out several mechanism test experiments beforehand, so as to obtain the connection between the control voltage, idle time, temperature change and other factors and the circuit breaker operating time [12]. Therefore, the workload is large, the robustness is poor, and it is not possible to implement the control of the movement process of the actuator mechanism to realize the adjustment of the contact movement speed and reduce the impact of pre-breakdown on the synchronous closure [13]-[15].

Modern intelligent heuristic algorithm is a very popular new discipline in recent years, which contains many disciplines such as artificial intelligence, information theory, cybernetics, etc., and solves many problems that are difficult to be solved in the field of traditional control [16]. Simulated annealing algorithm is a kind of global optimization algorithm, which is usually used to solve complex non-convex optimization problems. Its basic idea is to accept inferior solutions with a certain probability in order to avoid falling into local optimal solutions, so as to search for optimal solutions in the global range [17], [18]. Aiming at the shortcomings of permanent magnet switches, the simulated annealing algorithm is able to make the contacts move according to the given optimal reference trajectory to achieve the purpose of eliminating the influence of the control voltage, temperature change, mechanical aging and other factors [19], [20]. It is characterized by a wide search range, strong adaptability and high efficiency [21].

In this paper, an optimization design method of permanent magnet switch structure based on genetic algorithm and simulated annealing algorithm is proposed. Firstly, the working principle of the permanent magnet switch and the magnetic circuit model are introduced, and the finite element simulation model of the permanent magnet switch structure is designed by Infolytica MagNet simulation software. Secondly, from the perspective of multi-objective optimization, the multi-objective optimization model of the permanent magnet switch structure is established by taking the end height, eccentricity height, slamming time, energy conversion rate of slamming coil, cogging torque, and no-load airgap magnetic density waveform as the objective functions. Then a genetic algorithm is introduced to optimize the relevant parameters of the simulated annealing algorithm, and the optimization model of the permanent magnet switch structure is solved by the GA-SA algorithm. Finally, the feasibility of the algorithm to solve the optimization model is investigated through simulation examples, and the changes of the permanent magnet switch before and after the optimization as well as the relevant influencing factors are discussed.

II. Permanent magnet switch simulation modeling

In special fields such as aerospace, electric vehicles, and oil fields, not only does the permanent magnet drive motor (PMD) require high power density, but also high efficiency control puts higher demands on the performance of the motor. How to realize the effective control of permanent magnet switch under permanent magnet synchronous motor has become a research hotspot to improve the structure of permanent magnet synchronous motor.

II. A. Theory of permanent magnet switch

II. A. 1) Principle of operation of permanent magnet switches

Permanent magnetic switch technology is the use of magnetic materials, non-linear characteristics, according to the “inductance saturation impedance drops rapidly” this phenomenon, so that the permanent magnetic switch work in saturation and unsaturated core coil impedance non-linear change to control the capacitor charging and discharging different paths to achieve the effect of switching [22].

The permanent magnet switching compression network is shown in Fig. 1. All capacitors in the figure are equal, and the initial voltage of capacitor C_0 is U_0 switch S_0 is closed at $t = t_0$, at this time, C_0 is connected to C_1 through L_0, and as the resonant energy is transferred from C_0 to C_1, the voltage of both ends of the switch starts to rise. is transferred to C_1, when the voltage at the ends of C_1 starts to rise, the magnetic density inside the core of L_1 increases, and when the magnetic density inside the core reaches saturation density, the impedance of L_1 decreases rapidly. At this time the energy stored in capacitor C_1 starts to be transferred to capacitor C_2. If the saturation inductance of L_1 is much smaller than the value of the inductance of L_0, then the energy is transferred from C_1 to C_2 much faster than from C_0 to C_1. Thus energy compression is realized.

Figure 2 shows the magnetization curve of the core. Where L_1 is initialized to the point where B_r is left, when C_1 starts to be charged, the magnetic density in the core starts to grow along the magnetization curve from the point where B_r to $+B_{sat}$. If the magnetic switch L_1 is properly designed, then L_1 saturates just as the capacitor C_1 is charged to its maximum value. At this point, the impedance of the switch L_1 drops sharply causing a rapid discharge of capacitance C_1 to capacitance C_2. When the core is magnetized at the end of the current pulse, the core remanent magnetism is $+B_r$. This condition contradicts the condition that subsequent pulses require the correct operation of the magnetic switch because, at this point, the core will quickly reach saturation if it is magnetized again. Therefore, the system should be designed so that the magnetic density of the core material is “reset” to B_r before the next pulse is compressed, a process that is usually performed by a pulse or a DC current to reset the core to the proper position.

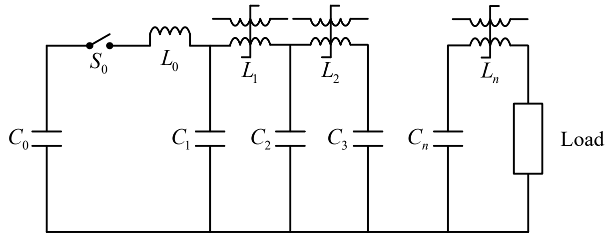

(a) Equivalent circuit of magnetic switch network

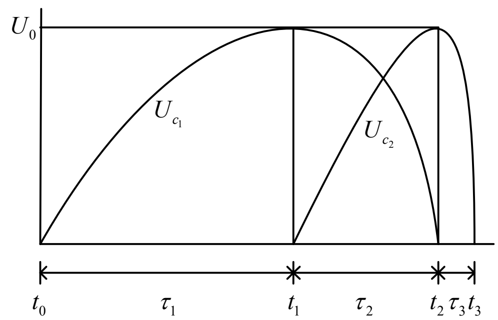

(b) Capacitor charging and discharging voltage waveforms

Figure 1: Permanent magnet switch compression network

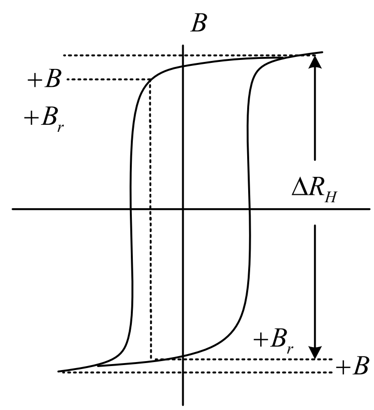

Figure 2: Core magnetization curve

The magnetic pulse compression network can be quantitatively described by analyzing the energy transfer and switching dynamics of the compression process at each level of the compression network. In order to facilitate the analysis, taking the ring permanent magnetic switch as an example, all circuit components are ideal cases, and in order not to lose the generality, the nth-order case is analyzed as follows:

The voltage across the capacitor at the saturation of the n th order magnetic switch can be expressed as:

$$V_{C_n}(t) = V_{C_{n-1}}(0)(1-\cos(\omega t))/2. \quad (1)$$

where V denotes the voltage of the capacitor L_{n-1} when the switch L_{n-1} is saturated, and $\omega=\frac{1}{\sqrt{L_n^{(s)}-1C_n/2}}$, with $L_{n-1}^{(s)}$ being the n^{-1} th order magnetic switch The saturation inductance C_n is the n th order capacitance, and in general, the saturation time of L_n is designed to coincide with the charging time of the capacitor C_n, which is dependent on the saturation reactance of L_{n-1}, and if the capacitance values of each stage are equal, then the C_n has a charging time of:

$$\tau_n = \pi\sqrt{L_{n-1}^{(s)}C_n/2} \quad (2)$$

It can be seen from the above equation, when all levels of magnetic switch saturation inductance value $L_n^{(s)}$ different at the same time, the saturation time of the magnetic switch is also different, and the pulse width at all levels are the sum of the charging and discharging time of the capacitor in the magnetic switch circuit, so with the level by level of $L_n^{(s)}$ decreases, the pulse width will be compressed continuously.

II. A. 2) Permanent magnet switch spurious parameters

n the magnetic pulse compression system, the equivalent inductance of the permanent magnet switch and its corresponding two-stage capacitance form a C-L-C resonant circuit to realize the energy transfer, and the output pulse is determined by the saturation inductance of the magnetic switch in the ideal case. However, in practice, stray resistance, stray inductance and stray capacitance will exist in the system. Since the saturation inductance of the permanent magnetic switch is very small, the presence of these stray parameters will limit the energy transfer time and reduce the energy transfer efficiency. Therefore, it is of great practical significance to optimize the design of stray parameters in magnetic pulse compression systems.

The stray resistance is mainly composed of the wiring resistance and the internal resistance of the magnetic switch winding. The surface resistance of the winding increases with the increase of the operating frequency, which causes the loss to increase. The energy loss of the magnetic switch winding also causes the local temperature of the magnetic switch core to rise, causing the hysteresis characteristics of the core to change. The stray resistance of the magnetic switch winding can be expressed as:

$$R_{stay} = \frac{\rho l}{\pi[r^2 - (r-\delta)^2]} \tag{3}$$

where ρ for the winding wire resistivity, l for the winding length, r for the winding conductor cross-section radius, δ for the skin depth. In the actual design process, you can choose a low resistivity, large cross-section radius of the winding conductor to reduce the magnetic switch stray resistance.

The permanent magnet switch winding can be equivalent to a nonlinear inductance, and when the core is switched from an unsaturated state to a saturated state, the equivalent inductance value will become smaller rapidly. Since the system transfers energy through C-L-C resonance, the presence of stray inductance increases the resonance time of the magnetic pulse compression circuit, resulting in a certain delay in the core saturation time, which has a large impact on the output pulse of the magnetic pulse compression system. The stray inductance can be expressed as:

$$L_{zxxy} = 0.2l(\ln(\frac{4l}{d}) - 0.75) \tag{4}$$

where l is the length of the wire and d is the cross-sectional diameter of the winding conductor. The design can reduce the magnetic switch's stray inductance by reducing the magnetic circuit length of the magnetic switch winding.

There are two types of stray capacitances in the ring structure of the permanent magnet switch: the turn-to-turn capacitance and the turn-to-turn shielding capacitance. In the actual design, try to make the distance between the permanent magnet switch and the wire small enough to make the turn-to-turn shielding capacitance negligible. The stray capacitance of the permanent magnet switch causes an increase in the time constant in the loop, which has an effect on the output waveform of the magnetic pulse compression system. The stray capacitance can be expressed as:

$$C_{zray} = \frac{\pi^2 D\varepsilon_0}{\ln(p/2r + \sqrt{(p/2r)^2 - 1})} \tag{5}$$

where D is the turn diameter, p is the winding pitch, r is the wire radius, and so is the relative dielectric constant. The more winding turns, the greater the inter-turn capacitance, and thus the greater the impact on the output waveform. The stray capacitance of the magnetic switch can be reduced by integrating the winding pitch and the number of winding turns.

II. B.Permanent magnet switch simulation model

II. B. 1) Magnetic Circuit Modeling of Permanent Magnet Switches

(1) Equivalent magnetic circuit model of permanent magnet

Currently commonly used permanent magnet switch materials include ferrite-type, aluminum cobalt-nickel-type, and neodymium-iron-boron (NdFeB) type, etc. Depending on the composition of the various materials, the permanent magnet switch materials generally have different hysteresis loops [23]. NdFeB permanent magnet switch materials are widely used in various permanent magnet switches due to their better hysteresis loop linearity and lower cost compared to AlCoNi-type permanent magnet switch materials. The hysteresis return line of NdFeB PM switch material can be simplified to a straight line after some equivalent treatment. Where B_r and H_c are the remanent magnetic density and coercivity of the permanent magnet, respectively.

From this, the magnetic density of the permanent magnet is related to the magnetic field strength as:

$$B = B_r - \frac{B_r}{H_c} H = B_r - \mu_0 \mu_r H \tag{6}$$

where μ_0 is the vacuum permeability, μ_r is the relative permeability of the permanent magnet, H is the external magnetic field strength, and B is the magnetic induction strength.

The above equation can be further can be transformed as:

$$\Phi = BS = B_r S - \frac{Hh_m}{\frac{h_m}{\mu_0 \mu_r S}} = \Phi_r - \frac{F}{R_m} \tag{7}$$

where Φ is the magnetic flux passing perpendicularly through the section S, Φ_r is the endowment flux of the permanent magnet, F is the magnetic pressure exerted on the external magnetic circuit, h_m is the length of the magnetization direction of the permanent magnet, and R_m is the internal magnetic resistance of the permanent magnet.

It is also possible to multiply both ends of the above equation by R_m together:

$$F = H_c h_m - \Phi R_m = F_r - \Phi R_m \tag{8}$$

where F_r is the endowed magnetic momentum of the permanent magnet.

(2) Equivalent magnetic circuit model of iron core

The core is mainly made of silicon steel sheets stacked with high permeability, the $B–H$ curve of silicon steel sheets is nonlinear, and it will enter the saturation state when the applied magnetic field strength is too large, which means that the slope of the $B–H$ curve decreases with the increase of H, so care should be taken to avoid the core from entering into the saturation region during the design process of the PMSLM. When the core is not saturated, it can be equated to a linear magnetoresistance R_{Fe}, i.e:

$$R_{Fe} = \frac{l}{\mu_0 \mu_{Fe} S} \tag{9}$$

where μ_{Fe} is the relative permeability of the core and l is the length of the magnetic circuit in that part of the core.

(3) Equivalent magnetic circuit model of air gap

The air gap of the permanent magnet switch is generally wide compared to the rotating motor, and the air gap itself is having a linear $B–H$ curve, so it can be simply equated to a linear air gap magnetoresistance R_δ as:

$$R_\delta = \frac{\delta}{\mu_0 \mu_{air} S} \tag{10}$$

where δ is the air gap length and μ_{air} is the relative permeability of air, generally taken as $\mu_{air} = 1$.

II. B. 2) Switch Simulation Modeling

With the continuous progress of science and technology and the rapid development of computer technology, it is more convenient to use the mathematical approximation method to simulate the real physical system of finite element analysis. The finite element not only has high computational accuracy, but also has strong adaptability to a variety of complex shapes, thus becoming one of the important analytical tools for electromagnetic field simulation of permanent magnet switch. The finite element analysis software that exists in recent years includes ANSYS, Maxwell, FEMTET, FLUX and Infolytica MagNet. In this paper, Infolytica MagNet is used to simulate the permanent magnet switch structure.

Figure 3 shows the finite element model of the permanent magnet switch based on Infolytica MagNet. When using the finite element method to analyze the magnetic field and performance of the permanent magnet switch, the settings of the finite element model pre-processing and the convergence judgment of the iterative solution will directly affect the solution accuracy, but the precise settings often require more detailed mesh sectioning, convergence accuracy, the number of iterations, etc., which will make the computational volume and the solution time greatly increased, so it is very important to set the appropriate pre-processing parameters in the finite element model of the permanent magnet switch. Therefore, it is very important to set appropriate pre-processing parameters in the finite element model of PM switch. In the pre-processing of MagNet, the Newton convergence accuracy is set to 0.01%, the conjugate gradient convergence accuracy is set to 0.01%, and the maximum number of Newton iterations is set to 50 times. For the permanent magnet switch, the electromechanical energy conversion is completed in the air gap, so the air gap mesh should be dissected more carefully, and the maximum edge length of the global mesh of the finite element model in this paper is 1.6 mm, and the maximum edge length of the air gap mesh is set to 0.4 mm.

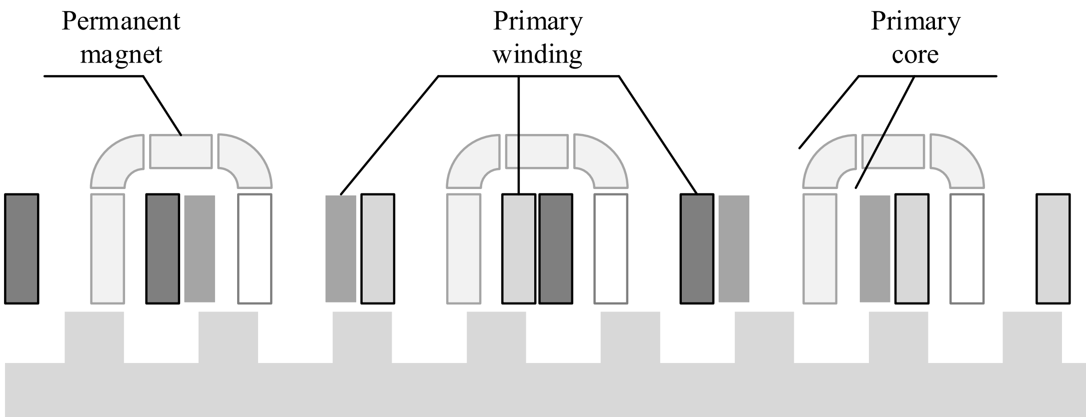

Figure 3: Finite element model of permanent magnet switch

III. Optimized design methodology for permanent magnet switches

In order to further enhance the electromechanical energy conversion efficiency and power of the permanent magnet linear motor, it is necessary to optimize the design of the permanent magnet switch structure, so as to ensure the practical application requirements of small amount of permanent magnets and simple secondary structure. Based on this, this paper introduces the simulated annealing algorithm and designs the optimization strategy of permanent magnet switch structure with multi-objective optimization, aiming to further enhance the application efficiency of permanent magnet linear motors.

III. A. Multi-objective optimization and algorithms

III. A. 1) Definition of multi-objective optimization

Multi-objective optimization problem (MOP) means that there is more than one decision variable, objective function, and constraints in the problem being dealt with, and with the different values of multiple decision variables, the results of the objective functions are different, and the optimality of one objective function is likely to cause the results of the other objective functions to be deteriorated. In the case of conflicting objective functions, the decision variables are output by coordinating the results of each objective function so as to achieve the global optimum [24].

The solution of multi-objective optimization problem is very different from single-objective optimization, there is no optimal solution, only relatively good solutions, and such solutions are generally multiple, or may be composed of infinitely many Pareto optimal solutions. In practical applications, a satisfactory solution should be selected from the Pareto-optimal solution according to the actual demand of the problem and the consideration of various factors such as cost.

The mathematical model of the MOP problem is expressed as follows:

$$\begin{cases} \min f(x) \\ g(x) \le 0 \end{cases} \tag{11}$$

where $f(x)=[f_1(x),...,f_m(x)]^T$, $m \geq 2$, is the dimension of the objective function, $g(x)=[g_1(x),...,g_p(x)]^T$, is the constraints, where p is the number of constraints, which contains equal or constraints or inequality constraints, and x is the n-dimensional decision variable. The above equation expresses to find the decision variable x for which the m-dimensional objective function $f(x)$ is the minimum within the feasible field $x \in D = \{x \mid g(x) \le 0\}$ of the system.

Against the above equation, the following concepts are introduced:

(1) Pareto domination. The solution x_1 dominates $x_2(x_1 \prec x_2)$ if and only if

$$f_i(x_1) \le f_i(x_2), i = 1,2...m \tag{12}$$

$$f_i(x_1) < f_i(x_2) \exists i \in (1,2...m) \tag{13}$$

(2) Pareto Optimality. A solution x_1 is Pareto optimal if and only if $\neg\exists x_2, x_2 \prec x_1$.

(3) Pareto optimal set. The set of all Pareto optimal solutions $P_s = \{x_1 \mid \neg\exists x_2; x_2 \prec x_1\}$.

(4) Pareto optimal front end. P_s The region formed by the corresponding objective function values in P_F is:

$$P_F = \{f(x) = (f_1(x), f_2(x), ..., f_m(x)) \mid x \in P_s\} \tag{14}$$

A solution is said to be non-dominated or non-inferior if it is not dominated by any of the solutions within its solution set. The multi-objective optimization algorithm is to find the current optimal solution, which is also a non-inferior solution, in each generation of the population, and the set formed by these optimal solutions is called the optimal solution set or non-inferior solution set. Then the solution set is updated through the optimization process, and finally the set approaches the Pareto optimal front end of the desired objective function, thus achieving optimization, and the output of the algorithm is the optimal solution set.

III. A. 2) Handling of relevant constraints

The related research proposes two constraint approach methods, the multi-objective optimization method and the penalty function method, to formulate the constrained optimization problem. Among them, the penalty function method constructs an objective function with a penalty term added to the fitness function, converts it into an unconstrained optimization problem, and penalizes the degree of constraint violation usually as a function individual particles. Their similarity is that they are both applicable to individual violation of constraints, and the difference is that the former takes the degree of individual violation of constraints as the objective function, plus the original objective function as an unconstrained multi-objective optimization problem.

In general, the multi-objective optimization problem is shown in Equation (11), and the global constraints are called constraints, which can be either equation constraints or inequality constraints. In the solution process, the equation constraints $h_j(x) = 0, j = 1,2,....,q$ needs to be changed to an inequality constraint by virtue of the following equation. Namely:

$$|h_j(x)| - \delta_j < 0, (\delta_j > 0) \tag{15}$$

δ_j is the j th equational constraint tolerance, usually taken as a very small positive number, and $\delta^* = (\delta_1, \delta_2, ..., \delta_q)$ is the equation constrained tolerance vector. Then Eq. (11) can be transformed into:

$$\min f(x) = (f_1(x), f_2(x), ..., f_m(x)) \\ s.t. \begin{cases} g_i(x) \le 0, i = 1,2,...,l \\ x \in R^n \end{cases} \tag{16}$$

where $x, f, f_k(x)$ is as defined above: $g_i : R^n \to R, (i = 1,2,...,l)$ denotes the i th constraint, $X = \{x \in R^n \mid g_i(x) \le 0, i = 1,2,...,l\}$ denotes the feasible domain of the decision variable.

III. A. 3) Simulated annealing optimization algorithm

Simulated Annealing (SA) algorithm is a Monte Carlo based stochastic optimization algorithm. In thermodynamics, annealing is a physical phenomenon that indicates that the energy state of a substance also increases when the temperature increases and decreases when the temperature decreases [25]. The core principle of annealing algorithm is to heat a solid from room temperature to high temperature and let it cool slowly. At room temperature, the object is in an amorphous state, after heating, the particles inside the solid start to become disordered and the internal energy gains an increase due to the increase in the ambient temperature, the process also eliminates any non-uniformity that may exist in the system and the subsequent cooling process can be restarted at a new equilibrium state. It is then allowed to cool down slowly, and when the temperature drops low enough, condensation and crystallization occurs, when the internal particles gradually tend to be arranged in an ordered state, which is in equilibrium under different circumstances. Finally when the temperature drops to room temperature, the internal energy of the particles will reach its lowest point.

According to statistical thermodynamics according to the principle of statistical thermodynamics, the energy distribution function P of the particles inside the object at a temperature of T can be expressed as:

$$p_a[E = E(\alpha)] = \frac{1}{Z(T)} \exp\left[-\frac{E(\alpha)}{K_a T} \right] \tag{17}$$

where $E(\alpha)$ is the energy of the state α , K_g is Boltzman's constant, and $Z(T)$ is the normalization factor.

The simulated annealing algorithm is an approximation for solving optimization problems with meritocracy and progressively lower tolerance for poor solutions. The initial state, the initial temperature, and the cooling rate are set to control the temperature drop, and the neighborhood structure of the solution space is used to search randomly to stabilize the energy and reach the equilibrium state. In the annealing procedure, the new state generated by the k+1st system improvement can be determined to be accepted or not according to the Metropolis acceptance principle, so as to achieve the best purpose, and its acceptance probability P can be expressed as:

$$P = \begin{cases} 1 & \Delta E \le 0 (\Delta E = E^{k+1} - E^k) \\ \exp\left[-\frac{E(\alpha)}{T} \right] & \Delta E > 0 \end{cases} \tag{18}$$

where T is the control parameter “temperature”.

The acceptance criterion for the corresponding state is:

$$P \ge RAN(1,0) \tag{19}$$

where $RAN(1,0)$ means that a random number is taken in (0, 1), and when the value of setting P is greater than or equal to the selected value, the two results are interchanged so that the state of the system changes. Conversely, the original state is maintained unchanged. The above operations are performed repeatedly until the number of consecutive unswapped numbers is greater than the set value or the temperature is reduced to the set value, and the system gradually reaches the global optimum as the number of operations increases.

III. B. Optimization of permanent magnet switch structure

III. B. 1) Optimized design of permanent magnet switches

According to the theory of “no free lunch”, no algorithm can solve different optimization problems at the same time, therefore, the development of optimization algorithms based on the structure of permanent magnet switches has become a kind of research topic. The optimal design of permanent magnet switch structure is essentially a problem of finding the maximum value of the objective function under the given constraints. The research objective of this paper is to find the minimum value, so the mathematical description of the permanent magnet switch structure optimization problem can be expressed as:

$$\begin{cases} \min f(X), X \in R^n \\ g_j(X) \le 0, j = 1, 2, \cdots, p \end{cases} \tag{20}$$

where $f(X)$ is the optimization objective function, $g(X)$ is the boundary constraints, X refers to the variables for optimization, n refers to the number of optimization variables, and p is the number of boundary constraints of the PM switch.

After clarifying the essential characteristics of the optimization of the permanent magnet switch structure, the optimization design of the permanent magnet switch structure problem is divided into the following steps:

(1) Choose a suitable optimization algorithm for motor optimization. The advantage of the global optimization algorithm is that the initial iteration position is randomly generated by a random function within the system rather than given by human beings, so less a priori knowledge is needed and the applicability of the algorithm will be stronger. The local search algorithm is mainly a local optimization search after the initial value is given. If the given initial range is reasonable, it is more likely to find the location of the optimal solution. Therefore, different optimization algorithms should be used for different optimization problems.

(2) Setting boundary conditions and determining optimization objectives and parameters for the permanent magnet switch structural model. The boundary conditions of the permanent magnet switch structure model are basically the constraints between physical dimensions. The iterative process of the optimization algorithm is to carry out a random scanning process within the definition domain of the given variables, and in the scanning process, it

is necessary to ensure that the structure of the permanent magnet switch does not overlap and that there are certain constraints between the dimensions.

(3) Build a joint simulation system combining the optimization algorithm and the Infolytica MagNet simulation model. In addition to writing the optimization algorithm, the optimization algorithm should be combined with the finite element simulation model, and MATLAB can generate the optimization algorithm into a script to control Infolytica MagNet to automatically build the model for simulation and data post-processing, and the whole process can be automated, so that the user can wait for the output result by clicking Start only once.

(4) Output the optimal results to compare the performance before and after optimization. After the optimization algorithm completes the iterative operation, the optimization algorithm will automatically give the final size results and final performance, and will also generate the simulation iteration number graph, through which we can see whether the algorithm has converged.

By scanning the algorithm, this paper selects six variables that have a greater impact on the output torque waveform. The optimization variables selected for this optimization design are six variable sizes, which are the end height, eccentric height, slamming time, slamming coil energy conversion rate, cogging torque, and no-load air-gap magnetic density waveform of the permanent magnet switch structure. The closing time and closing coil energy conversion rate of the permanent magnet switch structure are used as constraints to establish a multi-objective optimization model of the permanent magnet switch structure.

III. B. 2) Switch structure optimization process

Based on the SA algorithm and the optimization objective of the permanent magnet switch structure given in the previous section, this paper uses the SA algorithm optimized by genetic algorithm to solve the multi-objective optimization model of the permanent magnet switch structure with the following specific steps:

Step1 Input the maximum number of iterations, the initial value of the parameters related to the permanent magnet switch structure, the initial annealing temperature, the population size, the number of random seeds and other basic parameters.

Step2 Generate a set of random numbers to form the initial population according to the random seed and random number generator.

Step3 Decode the different populations, followed by the optimized variables, and merge them with the fixed variables into one scheme for the permanent magnet switch magnetic circuit calculation.

Step4 Calibrate the slot filling rate, if the slot filling rate does not meet the requirements, discard the scheme and return to Step3 to re-select a new scheme. Otherwise, proceed to the next step.

Step5 Calculate the fitness function.

Step6 Multi-objective convergence conditions judgment, if satisfied, then the algorithm ends to output the optimal solution, otherwise, proceed to the next step.

Step7 Select any two individuals in the population, perform crossover and mutation operations on these two individuals to generate two new individuals, find the fitness and acceptance probability of the two new individuals. If the acceptance probability is greater than the number of random seeds, the individual is accepted and the number of individuals is increased by 1. Otherwise, the individual is discarded and re-selected for cyclic calculation until the number of individuals in the sub-population increases to the number of populations.

Step8 Judge whether to reach the maximum number of iterations, if not, then modify the annealing temperature, the number of iterations plus 1, return to Step2, if reached, the next step.

Step9 Optimization end, output all non-inferior solutions.

IV. Optimized design simulation of permanent magnet switch

The optimization of permanent magnet switch structure helps to further enhance the control effect of permanent magnet motor, improve the power density of permanent magnet motor, and reduce the vibration noise of permanent magnet motor. Therefore, for the optimization strategy of permanent magnet switch structure proposed in this paper, this chapter carries out the simulation analysis, so as to provide reference for the optimization design of permanent magnet switch structure.

IV. A. Validation of the effectiveness of the GA-SA algorithm

IV. A. 1) GA-SA performance comparison

In the process of solving the optimization model of permanent magnet switch structure, this paper introduces the genetic algorithm to expand the population of the simulated annealing algorithm, which ensures that more non-inferior solutions can be retained, and then obtains the optimal optimization results of the permanent magnet switch structure. The initial settings of the simulated annealing algorithm are 0.85, 600 and 0.01 for the cooling rate, initial temperature and end temperature, respectively, and the chain length is set to 120, while the initial parameters of the classical genetic algorithm are set to 200 for the initial population, and the crossover probability and the mutation probability are 0.85 and 0.15, respectively, and the maximum number of evolutionary generations is 60. The maximum number of evolutionary generations of the quantum genetic algorithm (OGA) is set to 60, and the quantum gates are all quantum revolving gates with dynamically adjusted rotation angles, and the population size is 120.For the optimization performance of GA-SA, this paper selects a variety of different optimization algorithms to make comparisons, and the comparative results of its iterative evolutionary process are shown in Fig. 4.

As can be seen from the figure, the convergence efficiency of the simulated annealing algorithm is the lowest, and its optimal fitness value converges at about 2.87*105 after about 12 iterations, and the convergence values of the genetic algorithm and the quantum genetic algorithm are very close to each other, but the quantum genetic algorithm's convergence speed is better than that of the genetic algorithm. The improved GA-SA algorithm is better than other algorithms in terms of convergence speed and convergence efficiency, which to a certain extent shows that it is feasible to improve the simulated annealing algorithm by using the genetic algorithm, so that it possesses a better global search capability and convergence speed, which can lay a reliable algorithmic foundation for obtaining the optimal solution of the permanent magnet switch structure.

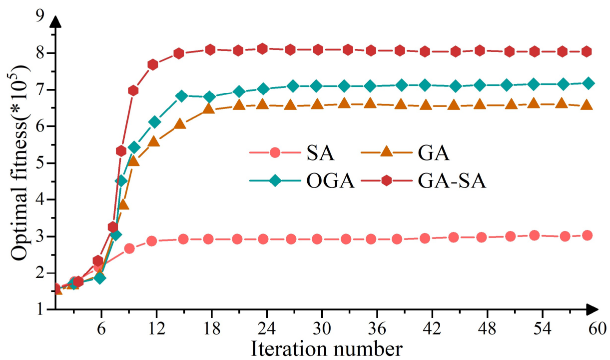

Figure 4: The comparison results of the iterative evolution process

IV. A. 2) Multi-objective optimization effect

The permanent magnet switch structure optimization problem in this paper is a typical MOP, using GA-SA algorithm for solving, this paper takes the cogging torque and the no-load airgap magnetic density waveform as an example for validation, and makes both of them reach a more desirable state through the reasonable combination of design variables. The expressions of the objective function of the MOP are set as in the previous section, based on which the degree of adaptation can be calculated. According to the steps of GA-SA to solve the optimization model of permanent magnet switch structure, the corresponding MATLAB program is written to complete the optimization process.

Running the written MATLAB program, the Pareto solution set generated after the optimization is shown in Fig. 5, where each solid point is a non-inferior solution. It can be seen that the distribution of each solution in the space is more uniform and the Pareto front end is well shaped.

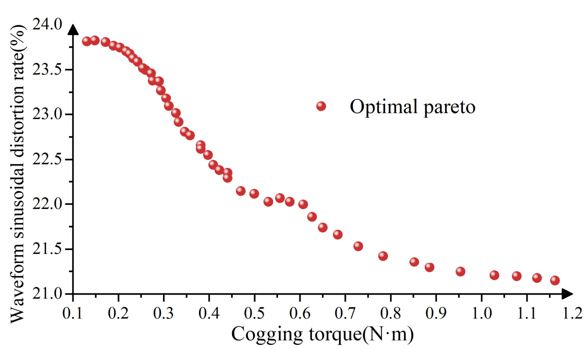

Figure 5: The final Pareto solution set

Each point in the figure corresponds to the respective values of the variables taken. In this paper, the permanent magnet switch structure is required to have a small cogging torque while maintaining a small sinusoidal distortion rate of the no-load air-gap magnetic density waveform, and the point in the middle of the graph is generally selected as the final solution. Meanwhile, the GA-SA algorithm essentially belongs to a random algorithm, so the set of Pareto solutions obtained after running the program each time will not be exactly the same. Three more reasonably shaped Pareto fronts are taken out, and 2 points are taken at a time for comparison. These 6 sets of values were brought into Infolytica MagNet in turn for simulation calculation, and the final results are shown in Table 1.

Comparing the six sets of results, it can be seen that the cogging torques calculated according to the optimized scheme are all relatively small, and at the same time, the corresponding waveform sinusoidal distortion rates are also relatively appropriate, which achieves the purpose of multi-objective optimization. In addition, the results calculated by the GA-SA algorithm are mostly close to those calculated by the finite element software, and the errors are between ±2.5%, which is within a reasonable range, and the accuracy of the GA-SA algorithm is continued in the multi-objective optimization of the permanent magnet switch structure. After comprehensive consideration, the point (0.74,4.08,0.77,9) is selected as the optimal solution point. The optimized cogging torque is 0.32N-m, and the sinusoidal distortion rate of the no-load air gap magnetic density waveform is 21.75%, which is a more ideal value in the design of the PM switch structure, and the PM switch structure under this parameter is in line with the operation requirements of the PM linear motor.

Table 1: The final result of multi-objective optimization

Pareto Solution	Cogging torque (N·m)		Waveform distortion (%)	
	Software	GA-SA	Software	GA-SA
Group 1	0.352	0.3598	22.52	22.6085
	0.657	0.6465	21.63	21.5129
Group 2	0.311	0.3102	22.58	22.0934
	0.324	0.3189	22.63	22.5735
Group 3	0.328	0.3411	22.45	22.7303
	0.276	0.2795	22.42	22.0643

IV. B. Comparison of simulation results before and after optimization

IV. B. 1) Changes in permanent magnet switch before and after optimization

In order to further verify the optimization effect of the selected optimal parameter level combinations on the optimization objectives of the permanent magnet switch structure, this paper uses the finite element simulation software to carry out dynamic simulation of the permanent magnet switch structure after optimization of the parameters, and obtains the changes in the values of the optimization objectives and constraint objectives before and after optimization, as shown in Table 2.

According to the calculation results, it can be seen that the tripping time is reduced by 14.09ms, the average tripping speed is increased by 21.92%, and the coil energy conversion rate is numerically increased by 5.92 percentage points, which is 20.80% compared with that before optimization. The closing time and closing coil energy conversion rate, which are the constraint objectives, are only slightly changed, with the closing time increasing by only 1.11ms, the average closing speed decreasing by 1.93%, and the coil energy conversion rate decreasing numerically by 0.79 percentage points, compared to the previous decrease of only 1.37%. This level parameter combination is satisfied if the closing time is taken to be no more than 4ms more than the original closing time as the constraint on the closing time and the closing coil energy conversion rate is not less than 50% as the constraint on the closing coil energy conversion rate. If the obtained constraint target does not satisfy the constraint conditions, according to the weight of the influence of each parameter variable on the constraint target in the simulation model of the permanent magnet switch, one more parameter with a larger influence on the constraint target should be selected, and the level value should be modified to be favorable to the constraint target and then be verified.

Table 2: optimization target value and constraint target before and after optimize

Optimize objectives	Opening time	Energy conversion rate of the opening coil
Before	64.27ms	28.46%
After	50.18ms	34.38%
Constraint objective	Closing time	Energy conversion rate of closing coil
Before	57.64ms	57.51%
After	58.75ms	56.72%

If only the tripping time and the energy conversion rate of the tripping coil are taken as the optimization objectives, but not the closing time and the energy conversion rate of the closing coil as the constraint objectives, according to the weight of the influence of each optimization variable on the tripping time and the energy conversion rate of the tripping coil in the simulation model of the permanent magnet switch, the optimal level combination at this time can be selected as (0.76,5.27,0.79,9). The results of the indicators obtained under this level combination are shown in Table 3.

According to the results, it can be seen that at this time, although the optimization of the two indexes of tripping time and tripping coil energy conversion rate is better, the closing time increases by 9.18ms, and the coil energy conversion rate decreases numerically by 13.82 percentage points, compared with the previous reduction of 24.03%. The increase of the closing time and the decrease of the closing coil energy conversion rate do not satisfy the constraints and are much larger than the results obtained when the optimization is carried out with the constrained objective, and they are also very close to the limit value of the closing time requirement of the permanent magnet switch, which is easy to fail to meet the requirements in practice, so the overall performance is not as good as that obtained when optimizing the two indexes of the closing time and the closing coil energy conversion rate as constrained objectives. From a comprehensive viewpoint, it is reasonable and necessary to optimize the closing time and closing coil energy conversion rate as the constraint objectives.

Table 3: optimization target value and constraint target before and after optimize

Optimize objectives	Opening time	Energy conversion rate of the opening coil
Before	64.27ms	28.46%
After	42.39ms	35.87%
Constraint objective	Closing time	Energy conversion rate of closing coil
Before	57.64ms	57.51%
After	66.82ms	43.69%

IV. B. 2) Effect of charging capacitor capacity

In the previous section, the optimization results of the permanent magnet switch structure under the four optimization objectives of slamming time, energy conversion rate of slamming coil, cogging torque and no-load air-gap magnetic density waveform were analyzed respectively, and then based on the optimized structural parameters of the permanent magnet switch, the influence of charging capacitance on the motion characteristics of the permanent magnet switch was simulated and analyzed, and then the change curves of electromagnetic repulsion, current, speed and displacement with time were obtained.

The initial capacitance capacity of the permanent magnet switch is set to 5mF, keeping the optimized permanent magnet switch structural parameters obtained in the previous section unchanged, and changing the capacitance capacities to 3mF, 5mF, 7mF, 9mF and 12mF, respectively.The simulation analyzes the influence of the charging capacitance capacity on the dynamic characteristics of the permanent magnet switch structure, and the simulation results are shown in Fig. 6. Among them, Fig. 6(a)~(d) shows the variation curves of electromagnetic repulsion, current, speed and displacement with time, respectively.

From the figure, it can be seen that the peak electromagnetic repulsive force increases significantly as the capacitance capacity increases, and the discharge current is the same. This indicates that when the capacitance capacity is small, the electromagnetic repulsive force is small and the time to maintain the peak electromagnetic repulsive force is also short. On the contrary, when the capacitance capacity is larger, to maintain the electromagnetic repulsion peak time is longer, but the electromagnetic repulsion rising speed is slower, is not conducive to rapid switching. Therefore, it is necessary to reasonably select the capacitance capacity in order to meet the design requirements of the mechanism. When the charging capacitance capacity is less than 5mF, the permanent magnet switch does not reach the full stroke opening distance within 2.3ms due to the lower speed, and the tripping fails. When the capacitance capacity is greater than 5mF, due to the faster speed, the mechanism has reached the full-stroke opening distance within 2.0ms, and the excessive speed will bring about mechanical impact, which puts forward higher requirements for the buffer device. Therefore, the capacitance capacity of 5mF is selected in this paper.It should be noted that in Fig. 6(a), the electromagnetic repulsion curves of 7mF, 9mF, and 12mF key capacitance capacities have inflection points at about 1.1ms, which can be ignored because the permanent magnet switch has already reached the maximum opening distance.

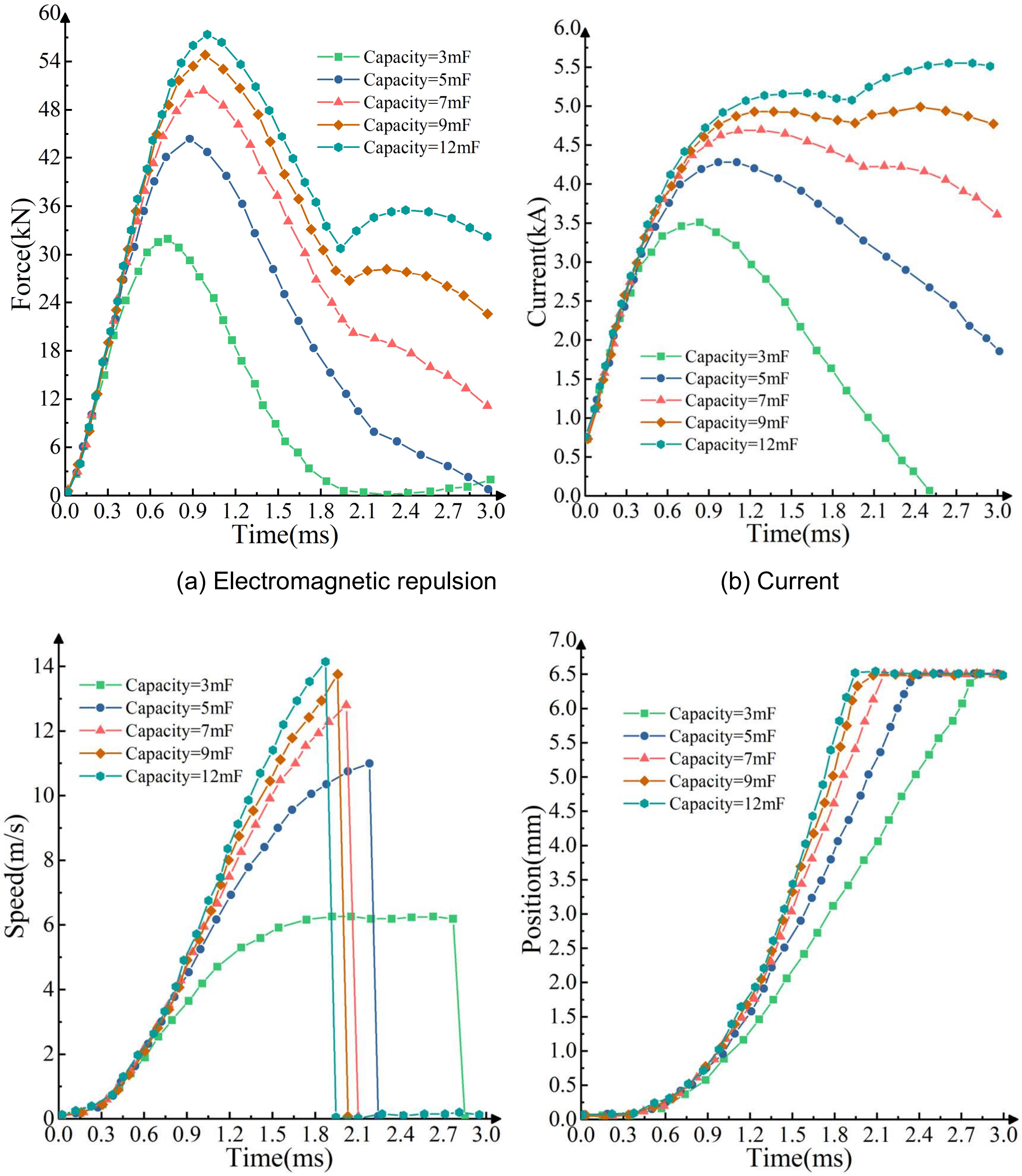

(a) Electromagnetic repulsion (b) Current

(c) Velocity (d) Displacement

Figure 6: The influence of the capacity of the charging capacitor

V. Conclusion

Based on the working principle and magnetic circuit model of the permanent magnet switch (PMS), the article establishes a simulation model of the PMS structure by combining with Infolytica MagNet simulation software. Starting from the multi-objective optimization problem of the permanent magnet switch structure, the corresponding objective function and constraints are set, and the simulated annealing algorithm improved by genetic algorithm is used to solve the problem, so as to obtain the optimal parameters of the permanent magnet switch structure. The simulation results show that it is feasible to use GA-SA algorithm to solve the optimization model of permanent magnet switch structure, and the overall computational efficiency is high. The opening time and the energy conversion rate of the opening coil of the optimized PM switches are significantly improved, and the closing time and the energy conversion rate of the closing coil do not change significantly. In addition, the charging capacitance capacity will have a certain impact on the permanent magnet switch structure, so it is necessary to comprehensively consider the impact of the charging capacitance capacity when setting the permanent magnet switch structure, so as to ensure the efficient and stable operation of the permanent magnet linear motor.

References

[1] Liu, Y., Dang, D., & Lee, S. K. (2024). Research on the Protection System for Smart Grid Based on Phasor Information at Circuit Breakers. Energies, 17(14), 3455.

[2] Radmanesh, H., & Kavousi, A. (2017). Aircraft electrical power distribution system protection using smart circuit breaker. IEEE Aerospace and Electronic Systems Magazine, 32(1), 30-40.

[3] Pan, P., & Mandal, R. K. (2024). Intelligent short-circuit protection with solid-state circuit breakers for low-voltage DC microgrids. IETE Journal of Research, 70(3), 3187-3203.

[4] Xie, Z., Hou, L., He, P., Cai, Y., & Wang, Y. (2025). Accelerated Degradation Test and Performance Degradation Characteristics of Intelligent Circuit Breaker Control Circuit. Processes, 13(5), 1340.

[5] Alizadeh, M., Li, X., Wang, Z., Scaglione, A., & Melton, R. (2012). Demand-side management in the smart grid: Information processing for the power switch. IEEE Signal Processing Magazine, 29(5), 55-67.

[6] Liu, S., Chen, B., Zourntos, T., Kundur, D., & Butler-Purry, K. (2014). A coordinated multi-switch attack for cascading failures in smart grid. IEEE Transactions on Smart Grid, 5(3), 1183-1195.

[7] Li, Y., & Yan, J. (2022). Cybersecurity of smart inverters in the smart grid: A survey. IEEE Transactions on Power Electronics, 38(2), 2364-2383.

[8] Hou, C., Yu, X., Cao, Y., Lai, C., & Cao, Y. (2017). Prediction of synchronous closing time of permanent magnetic actuator for vacuum circuit breaker based on PSO-BP. IEEE Transactions on dielectrics and Electrical Insulation, 24(6), 3321-3326.

[9] Zhang, Z., Tian, G., Li, B., & Qin, H. (2024, July). Design of a Synchronous Control System for Permanent Magnet Vacuum Circuit Breakers Based on Improved Genetic Algorithm. In 2024 3rd International Conference on Artificial Intelligence and Autonomous Robot Systems (AIARS) (pp. 67-72). IEEE.

[10] Peng, J., & Wang, X. (2022). An Intelligent Control‐Based Vacuum Circuit Breaker with Permanent Magnet and Dynamic Characteristic Analysis. Mobile Information Systems, 2022(1), 8086231.

[11] Fang, S., Liu, Q., Lin, H., & Ho, S. L. (2015). A novel flux-weakening control strategy for permanent-magnet actuator of vacuum circuit breaker. IEEE Transactions on Industrial Electronics, 63(4), 2275-2283.

[12] Su, Y., Zhou, K., Huang, W., Lu, Y., Peng, Y., & Hong, G. (2024, September). Review on control algorithm of drive system of permanent magnet synchronous motor for high voltage circuit breaker. In 2024 6th International Conference on Energy, Power and Grid (ICEPG) (pp. 1545-1550). IEEE.

[13] Yang, S. L., & Zeng, L. G. (2014). The Design of the Permanent Magnet Vacuum Circuit Breaker Control System Based on SOPC. Applied Mechanics and Materials, 530, 1036-1042.

[14] Lou, J., Liu, A., & Yu, S. (2019). A reliable and controllable motor actuator without permanent magnetic for 40.5 kV vacuum circuit breakers. IEEE Transactions on Industry Applications, 56(2), 1218-1225.

[15] Li, Y., Kang, Y., Wang, T., Guo, L., Wang, H., & Wang, H. (2017, August). Dynamic characteristics research on single phase permanent magnet swing angle torque motor of high voltage vacuum circuit breaker. In 2017 IEEE Transportation Electrification Conference and Expo, Asia-Pacific (ITEC Asia-Pacific) (pp. 1-5). IEEE.

[16] Desale, S., Rasool, A., Andhale, S., & Rane, P. (2015). Heuristic and meta-heuristic algorithms and their relevance to the real world: a survey. Int. J. Comput. Eng. Res. Trends, 351(5), 2349-7084.

[17] Pardalos, P. M., & Mavridou, T. D. (2024). Simulated annealing. In Encyclopedia of Optimization (pp. 1-3). Cham: Springer International Publishing.

[18] Rere, L. R., Fanany, M. I., & Arymurthy, A. M. (2015). Simulated annealing algorithm for deep learning. Procedia Computer Science, 72, 137-144.

[19] Chen, W., Chen, J., Sun, H., & Chen, Z. (2019). Simulation and analysis of irregular multicoil B 0 shimming in C-type permanent magnets using genetic algorithm and simulated annealing. Applied Magnetic Resonance, 50, 227-242.

[20] Rama, R. S., Edwin Selva Rex, C. R., Anantha Rufus, N., & Annrose, J. (2023). THD Reduction for Permanent Magnet Synchronous Motor Using Simulated Annealing. Intelligent Automation & Soft Computing, 35(2).

[21] Su, G., Wang, P., Guo, Y., Cheng, G., Wang, S., & Zhao, D. (2022). Multiparameter identification of permanent magnet synchronous motor based on model reference adaptive system—Simulated annealing particle swarm optimization algorithm. Electronics, 11(1), 159.

[22] Ullah Wasiq,Khan Faisal,Sulaiman Erwan,Sami Irfan & Ro Jong Suk. (2021). Analytical Sub-Domain Model for Magnetic Field Computation in Segmented Permanent Magnet Switched Flux Consequent Pole Machine. IEEE ACCESS,9,3774-3783.

[23] Fengrui Cui,Junquan Chen,Pengfei Hu,Xingyu Wu & Fangxu Sun. (2025). An Equivalent Magnetic-Circuit-Modeling Approach for Analysis of Conical Permanent Magnet Synchronous Motor. Sensors,25(6),1788-1788.

[24] Zhe Liu,Fei Han,Qinghua Ling,Henry Han,Jing Jiang & Qing Liu. (2025). A multi-objective evolutionary algorithm based on a grid with adaptive divisions for multi-objective optimization with irregular Pareto fronts. Applied Soft Computing,176,113106-113106.

[25] Qinjin Zhang,Liming Song,Yji Zeng,Yancheng Liu,Siyuan Liu & Ning Wang. (2025). Real-time power optimization strategy for fuel cell ships based on improved genetic simulated annealing algorithm. Electric Power Systems Research,245,111647-111647.